Fischer-Tropsch Synthesis Product Grade Optimization in a Fluidized Bed Reactor

Fabiano A. N. Fernandes and Elida M. M. Sousa
Universidade Federal do Ceara, Departamento de Engenharia Quimica, Campus Universitario do Pici, Bloco 709, 60455-760 Fortaleza - CE, Brazil

DOI 10.1002/aic.10887
Published online June 5, 2006 in Wiley InterScience (www.interscience.wiley.com).

Fischer-Tropsch synthesis is an important chemical process for the production of liquid fuels and olefins. In recent years, the abundant availability of natural gas and the increasing demand of olefins, gasoline, diesel and waxes have led to a high interest in further developing this process. A mathematical model of a fluidized-bed reactor used for syngas polymerization was developed and the carbon monoxide polymerization was studied from a modeling point of view. Simulation results show that several parameters affect syngas conversion and carbon product distribution, such as operating pressure, superficial gas velocity, bed porosity, and syngas composition. Optimization of liquid hydrocarbon products was done and the best operating conditions for their production were found for an iron catalyst that produces hydrocarbon chains according to a dual mechanism theory. © 2006 American Institute of Chemical Engineers *AIChE J,* 52: 2844–2850, 2006
Keywords: fluidized-bed reactor, Fischer-Tropsch, modeling, optimization

Introduction

The Fischer-Tropsch synthesis (FTS) was discovered nearly 80 years ago, but up until now its application in producing liquid fuels and other chemicals has not been fully explored especially due economical reasons. In recent years, the escalate in oil prices made the FTS a subject of renewed interest particularly in converting natural gas into liquid transportation fuels. Natural gas can be converted to carbon monoxide and hydrogen (synthesis gas) via the existing processes, such as steam reforming, carbon dioxide reforming, partial oxidation and catalytic partial oxidation, followed by the FT synthesis reaction

$$CO + 2H_2 \rightarrow (—CH_2—) + H_2O \quad (1)$$

When iron catalysts are used, the carbon monoxide polymerization occurs in combination with the water gas shift reaction (WGS)

$$CO + H_2O \leftrightarrow CO_2 + H_2 \quad (2)$$

Many researchers have been working on catalyst development,[1,2] reactor design,[3-6] and on the commercial applications of the Fischer-Tropsch synthesis,[7,8] but few investigations have been done in order to optimize production of specific products. The FT synthesis yields predominantly straight hydrocarbons chains (α-olefins and paraffins), and there is a general agreement that the reaction may be viewed as a methylene polymerization reaction where the methylene monomer unit ($= CH_2$) is not initially present. Hydrogenation of CO generates the methylene monomer *in situ*, and polymerization occurs through addition of methylene units in the growing hydrocarbon chain. The polymerization steps involved in the FT synthesis are: initiation of chains, competing chain propagation and chain termination. The product distributions tend to obey the Anderson-Shultz-Flory chain-length statistics, but this is not always true, and many researchers have reported deviations from the ASF theory.[9-11] Theories for ASF deviations are based in the superposition of two ASF distributions and relay in the dual site theory,[11] secondary chain growth of readsorbed alkenes theory,[9,10] and the dual mechanism of chain growth theory.[12,13] Iron catalysts are more likely to obey a dual mechanism of

Correspondence concerning this article should be addressed to F. A. Fernandes at fabiano@efftech.eng.br.

chain growth theory. In this work a mathematical model of a fluidized-bed reactor used for syngas polymerization was developed, and the carbon monoxide polymerization was studied from a modeling point of view, based on the kinetics of an iron catalyst, which obeys to a dual mechanism theory. Optimization of gasoline and diesel were done in order to search for the best operating conditions for their production.

Fluidized-Bed Reactor

The fluidized-bed reactor for hydrocarbon production comprises of two different phases. Syngas and inert gases are fed into the bottom of the reactor through a distributor, and split to form the bubble and the emulsion phases. The excess gas not needed for maintaining the minimum fluidization condition passes through the bed as bubbles. Nonreacted gases exiting from the top of the fluidized bed flow upward through a disengaging zone in the upper part of the reactor. The disengaging zone is normally larger in diameter than the catalytic bed zone as to reduce the gas flow velocity and, thereby, facilitate the settling of solid particulate (catalyst). Particles that pass through the disengaging zone are separated from the gas phase by mean of a cyclone and are then returned to the fluidized bed.

The catalyst is generally fed in near the top of the reactor. As the reaction proceeds, hydrocarbons are formed on the catalyst surface. During operation of the reactor, hydrocarbons are continuously formed and the product is removed from the reactor with the nonreacted syngas. In the reactor, cooling tubes are provided to remove the heat released by the FT reaction and to control the reactor temperature, ensuring the isothermal conditions inside the reactor, despite the high heat of reaction (ΔH = - 170 kJ/mol CO).

Mathematical Model

Fluidized-bed reactor model

The model developed in this work is a two-phase heterogeneous model for the fluidized-bed reactor used in polymerization reactions. Besides the common assumptions for fluidized-bed reactor models (the polymerization reaction occurs only in the emulsion phase, the emulsion phase is at its minimum fluidizing condition, gas in excess of that required for maintaining minimum fluidization conditions passes through the bed as bubbles, and bubbles grow only to a maximum stable size and travel up the reactor in plug-flow regime), the following additional assumptions were made in the development of the pseudo-heterogeneous model: the emulsion phase is assumed to be well-mixed; particles are assumed to have a constant diameter; radial concentration gradient, radial temperature gradient and elutriation of catalyst particles are assumed to be negligible.

The overall kinetic rates for the FT reaction on an iron catalyst,[1] and for the WGS reaction[1] are given by

$$R_{\mathrm{FTS}} = \frac{k_{\mathrm{FTS}} \cdot P_{\mathrm{CO}} \cdot P_{\mathrm{H2}}}{(P_{\mathrm{CO}} + a \cdot P_{\mathrm{H2O}})} \tag{3}$$

$$R_{\mathrm{WGS}} = \frac{k_{\mathrm{WGS}} \cdot \left(P_{\mathrm{CO}} \cdot P_{\mathrm{H2O}} - \dfrac{P_{\mathrm{CO2}} \cdot P_{\mathrm{H2}}}{K_1}\right)}{(P_{\mathrm{CO}} + K_2 \cdot P_{\mathrm{H2O}})^2} \tag{4}$$

Material balance of the emulsion phase assumes the consumption of gas during the Fischer-Tropsch synthesis and the mass transfer between bubble and emulsion phases by diffusion (Eq. 5). The emulsion gas phase energy balance consists of energy transfer due to the temperature gradient between the emulsion phase and the bubble phase, energy transfer by the diffusing gases, and due to the heat released by the exothermal reaction (Eq. 6)

$$C_{e,i} = C_{0,i} + \frac{H \cdot \rho_P \cdot (1-\varepsilon) \cdot \Sigma\,(\nu_j \cdot R_j)}{V_e \cdot U_e \cdot \varepsilon} - \frac{H \cdot \delta \cdot Km_i \cdot (\overline{C_{b,i}} - C_{e,i})}{U_e \cdot (1-\delta) \cdot \varepsilon} \tag{5}$$

$$T_e = T_0 - \frac{H \cdot [c^*_{pg} \cdot Km \cdot (\Sigma\, C_{b,i} - \Sigma\, C_{e,i}) + Hm] \cdot (T_b - T_e) \cdot \delta}{U_e \cdot (1-\delta) \cdot \varepsilon \cdot c^*_{pg} \cdot \Sigma\, C_{e,i}} + \frac{(1-\varepsilon_{mf}) \cdot H \cdot \Sigma\, R_j \cdot [-\Delta H_j - (c_{ps} - c_{pg}) \cdot (T_e - T_{\mathrm{ref}})]}{U_e \cdot \varepsilon \cdot c^*_{pg} \cdot \Sigma\, C_{e,i}} \tag{6}$$

Mass transfer between bubble phase and emulsion gas phase occurs by diffusion through bubble clouds (Eq. 7). Energy transfer between phases occurs due to the temperature gradient between the phases and also by the diffusion of gases (Eq. 8)

$$\frac{dC_b}{dz} = -\frac{Km \cdot (C_{b,i} - C_{e,i})}{U_b} \tag{7}$$

$$\frac{dT_b}{dz} = \frac{H_m}{U_b \cdot C_b \cdot c^*_{pg}} \cdot (T_b - T_e) \tag{8}$$

The boundary conditions at the reactor entrance: z = 0 $\rightarrow$ $C_{0,i} = C_{e,i} = C_{b,I}$ and $T_0 = T_b = T_e$. The correlations used to predict the bubble fraction in the bed, bubble and emulsion phases gas velocity, voidage of the emulsion phase, material and heat-transfer coefficients and maximum stable bubble size are listed in Table 1.

To solve the mathematical model, first, initial estimates were provided for the gas concentration and temperature in the emulsion phase (step 1). These values were used to numerically integrate Eqs. 7 and 8 (step 2), and after that to solve the algebraic Eqs. 5 and 6 (step 3), obtaining new values for gas concentration in the emulsion phase. An iterative procedure was created to run steps 2 and 3 till the concentrations in all phases converged. The numerical integration was carried out using a 5$^{\mathrm{th}}$ order Runge-Kutta method. The kinetic parameters for the reaction are presented in Table 2, the operating conditions used in the simulations are presented in Table 3, and the gas properties are presented in Table 4. The overall kinetic rates for the Fischer-Tropsch reaction and the WGS reaction were taken from Raje and Davis[1].

Kinetic model

The kinetic model used to simulate the CO polymerization and product distribution assumes that the alkyl and alkenyl mechanisms act together in the FT synthesis.

Table 1. Correlations used in the Model

Emulsion phase volume	$V_e = V_R \cdot (1 - \delta)$
Bubble phase volume	$V_b = V_R \cdot \delta$
Minimum fluidizing velocity[14]	$\frac{1.75}{\varepsilon_{mf}^3} \cdot \mathrm{Re}_{mf}^3 + \frac{150 \cdot (1 - \varepsilon_{mf})}{\varepsilon_{mf}^3} \cdot \mathrm{Re}_{mf} - Ar = 0$
	$\mathrm{Re}_{mf} = (29.5^2 + 0.0357 \cdot Ar)^{0.5} - 29.5$
	$Ar = \frac{d_p^3 \cdot \rho_g \cdot (\rho_p - \rho_g) \cdot g}{\mu_g^2}$
Emulsion velocity[15]	$U_e = \frac{U_{mf}}{\varepsilon_{mf} \cdot (1 - \delta)}$
Bubble velocity[16]	$U_b = U_0 - U_{mf} + 0.711 \cdot (g \cdot d_b)^{0.5}$
Bubble fraction (voidage)[17]	$\delta = \frac{U_0 - U_{mf}}{U_b}$
Mass interchange[17]	$\frac{1}{K_m} = \frac{6}{d_b} \cdot \left(\frac{1}{K_{bc}} + \frac{1}{K_{ce}}\right)$
	$K_{bc} = 4.5 \cdot \frac{U_{mf}}{d_b} + 10.4 \cdot \left(\frac{D^{0.5}}{d_b^{1.5}}\right)$
	$K_{ce} = 6.78 \cdot \left(\frac{\varepsilon_{mf} \cdot D \cdot U_b}{d_b^3}\right)^{0.5}$
Heat interchange[17]	$\frac{1}{H_m} = \frac{6}{d_b} \cdot \left(\frac{1}{H_{bc}} + \frac{1}{H_{ce}}\right)$
	$H_{bc} = 4.5 \cdot \frac{U_{mf} \cdot \rho_g \cdot c_{pg}}{d_b} + 10.4 \cdot \left(\frac{k_g \cdot \rho_g \cdot c_{pg}}{d_b^{2.5}}\right)^{0.5}$
	$H_{ce} = 6.78 \cdot (\rho_g \cdot c_{pg}^* \cdot k_g)^{0.5} \cdot \left(\frac{\varepsilon_{mf} \cdot U_b}{d_b}\right)^{0.5}$
Porosity[18]	$\varepsilon_{mf} = 0586 \cdot \phi^{-0.72} \cdot \frac{1}{Ar^{0.029}} \cdot \left(\frac{\rho_g}{\rho_p}\right)^{0.021}$
Bubble diameter[19]	$d_b = d_{bm} - (d_{bm} - d_{bo}) \cdot e^{-0.3 \cdot H/2D}$
	$d_{bm} = 0.652[A(U_0 - U_{mf})]^{0.4}$
	$d_{bo} = 0.00376(U_0 - U_{mf})^2$

The alkyl mechanism can be represented by the following reactions

$$\cdot CH_2 + \cdot H \xrightarrow{ki1} R(1) \quad \text{initiation}$$

$$R(n) + \cdot CH_2 \xrightarrow{kp1} R(n+1) \quad \text{propagation}$$

$$R(n) + \cdot H \xrightarrow{k\text{par}} P(n) \quad \text{reduction by surface hydride giving an alkane}$$

$$R(n) \xrightarrow{k\text{olef}} P^{=}(n) \quad \beta\text{-hydride elimination giving an olefin (termination)}$$

The alkenyl mechanism can be represented by the following reactions

$$\cdot CH_2 + \cdot CH \xrightarrow{ki2} R(2) \quad \text{initiation}$$

$$R''(n) + \cdot CH_2 \xrightarrow{kp2} R''(n+1) \quad \text{propagation}$$

$$R''(n) \xrightarrow{k\text{olef 2}} P^{=}(n) \quad \text{reduction giving an olefin (termination)}$$

The population balance for the FTS species are given by the following set of equations

$$R(1) = \frac{k_i \cdot P_{H2}}{k_p} \tag{9}$$

$$R''(2) = \frac{k_{i2} \cdot R_{FTS}}{k_{p2}} \tag{10}$$

$$R(n) = \frac{k_p \cdot R_{FTS}}{k_p \cdot R_{FTS} + k_{par} \cdot P_{H2} \cdot k_{olef}} \cdot R(n-1) \tag{11}$$

$$R''(n) = \frac{k_{p2} \cdot R_{FTS}}{k_{p2} \cdot R_{FTS} + k_{olef\ 2}} \cdot R''(n-1) \tag{12}$$

$$\frac{dP(1)}{dt} = k_{met} \cdot P_{H2} \cdot R(1) \tag{13}$$

$$\frac{dP(2)}{dt} = k_{et} \cdot P_{H2} \cdot R''(2) \tag{14}$$

Table 2. Kinetic Parameters for Fischer-Tropsch Synthesis in Iron Catalyst and for Water Gas Shift[1]

k_{FTS}	0.1106 [mol/kg · s · MPa]
a	3.016
k_{WGS}	0.0292 [mol/kg · s]
K_1	85.81
K_2	3.07

Table 3. Operating Conditions and Reactor Parameters

Gas superficial velocity [m/s]	0.40 to 0.60
Total pressure [MPa]	1.0 to 3.0
Temperature [°C]	270
Reactor height [m]	10.0
Reactor diameter [m]	3.0
Reactor bed porosity	0.85 to 0.95
Catalyst particle diameter [m]	0.0002 to 0.0003
Catalyst apparent density [kg/m^3]	957.0

Table 4. Gas Properties

CO diffusivity [m^2/s]	17.2×10^{-9}
H_2 diffusivity [m^2/s]	45.5×10^{-9}
CO_2 diffusivity [m^2/s]	24.9×10^{-9}
H_2O diffusivity [m^2/s]	31.7×10^{-9}
Gas mixture density [kg/m^3]	1.20
Gas mixture viscosity [kg/m · s]	1.80×10^{-5}

Table 5. Kinetic Parameters for CO Polymerization in Iron Catalyst (at 270°C)

k_i [MPa^{-1}]	0.4963
k_{i2} [h · mol^{-1}]	8.054
k_p [mol^{-1}]	0.3530
k_{p2} [mol^{-1}]	0.4206
k_{par} [MPa^{-1} · h^{-1}]	0.02314
k_{olef} [h^{-1}]	0.003487
k_{olef2} [h^{-1}]	0.04792
k_{met} [MPa^{-1} · h^{-1}]	0.06386
k_{et} [MPa^{-1} · h^{-1}]	0.02421
k_{O2} [h · mol^{-1}]	0.09994

$$\frac{dP^{=}(2)}{dt} = k_{O2} \cdot R_{FTS}^2 \tag{15}$$

$$\frac{dP(n)}{dt} = k_{par} \cdot P_{H2} \cdot R(n) \tag{16}$$

$$\frac{dP^{=}(n)}{dt} = k_{olef} \cdot R(n) + k_{olef\,2} \cdot R''(n) \tag{17}$$

The development of the population balances assumes that the quasi-steady state is applied to the propagating species (as commonly assumed for the moments of live polymers); the consumption of methylene units is proportional to the overall reaction rate; and the concentration of hydrogen in the polymerization site is proportional to the partial pressure of hydrogen in the reaction media. The details on the development of the population balances for the FT synthesis for this specific catalyst (Fe:0.005K:21.7Si) can be found in Fernandes[20]. The kinetic parameters for the CO polymerization are presented in Table 5.

The model has been validated using the data reported by Raje and Davis[1] and Donnelly and Satterfield[21] and has provided a satisfactory fitting[20] (samples are shown in Figure 1). Variance analysis was done using the software Statistica 6.0 which showed that the model is significant within 1% of confidence. For the sample shown in Figure 1a, the regression R^2 for paraffin and olefin was, respectively, 0.999 and 0.955. F-test presented the values of 6596 for paraffin, and 148 for olefin which are more than 3 times the listed F values (11.26 and 12.25 for 1% of confidence, respectively, for paraffin and olefin) guaranteeing that the model is very significant. For the sample shown in Figure 1b, the regression R^2 for paraffin and olefin was, respectively, 0.996 and 0.975. F-test presented the values of 2067 for paraffin and 271 for olefin, which are more than 3 times the listed F values (11.26 and 12.25 for 1% of confidence, respectively, for paraffin and olefin). Total hydrocarbon number of moles was also tested and returned a regression R^2 of 0.994, and a F value of 1278, also more than 3 times the listed F value (8.53 for 1% of confidence level).

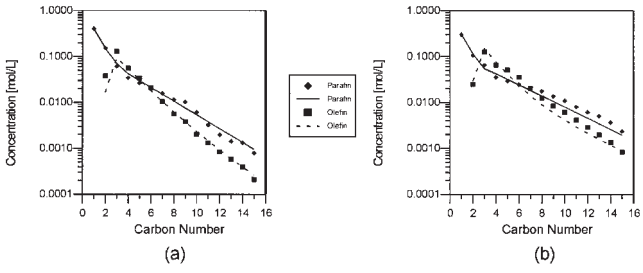

Figure 1. Carbon number distributions of paraffin and olefin products for: (a) H_2:CO = 0.67, P_T = 1.3 MPa, T = 270°C and (b) H_2:CO = 1.70, P_T = 1.3 MPa, T = 270°C.

Symbols refer to experimental data and lines to model simulation results.

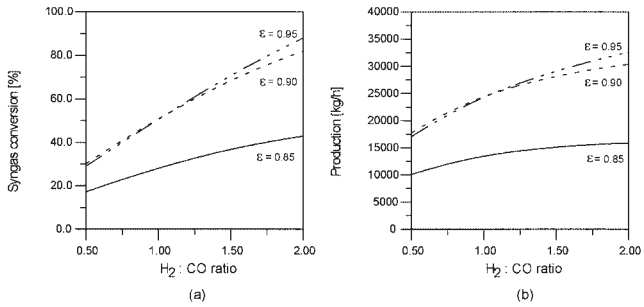

Figure 2. Syngas conversion into hydrocarbons (a), and reactor productivity (b), as function of H_2:CO ratio for three different bed porosities (conditions: 2.0 MPa, 270°C, U_0 = 0.6 m/s).

Results and Discussion

Fischer-Tropsch synthesis in fluidized bed reactors is a very complex system with many process variables that should be accounted for: superficial gas velocity, emulsion velocity, bed porosity, total pressure and H_2:CO ratio. The results of the simulations performed with the reactor model described above are presented here. The influence of the superficial gas velocity, bed porosity, operating pressure and H_2:CO ratio, on syngas conversion, total reactor productivity and product selectivity, especially in the range of gasoline and diesel, were studied. Simulations were carried out for a range of superficial gas velocities U_0 = 0.40 – 0.60 m/s, while bed porosity range was ε = 0.85 – 0.95, operating pressure range was P_T = 1.0 – 3.0 MPa, and H_2:CO ratio was 0.5 – 2.0. The main results of the simulations are reported in Figures 2–6.

Increasing the inlet superficial gas velocity causes a decrease in conversion of syngas into hydrocarbons, and in reactor productivity. Increasing H_2:CO ratio in the gas inlet and in-

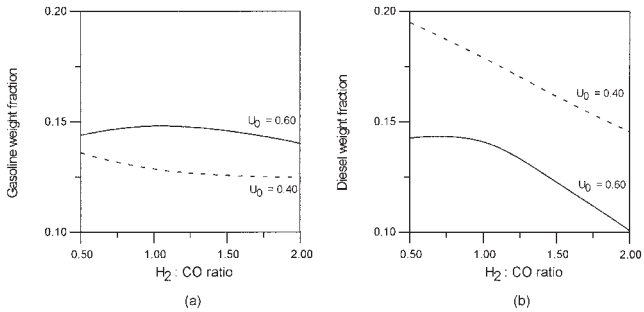

Figure 3. Weight fraction of (a) gasoline; and (b) diesel for two different superficial gas velocities (conditions: 2.0 MPa, 270°C, ε = 0.85).

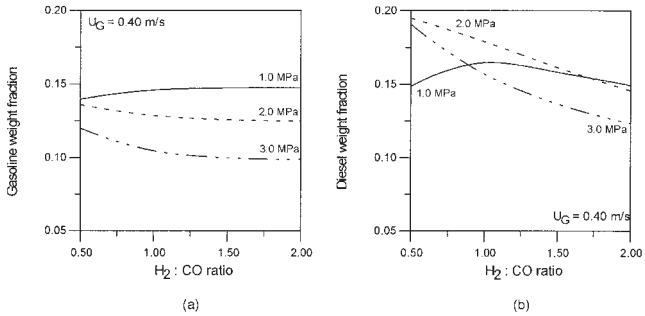

Figure 4. Weight fraction of (a) gasoline; and (b) diesel for three operating pressures (conditions: 270°C, U_0 = 0.4 m/s, ε = 0.85).

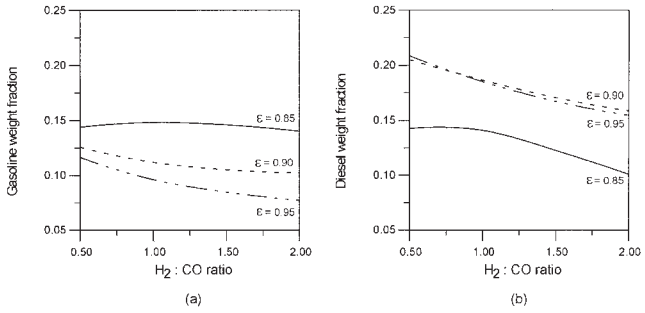

Figure 6. Weight fraction of (a) gasoline; and (b) diesel for three different reactor bed porosities (conditions: 2.0 MPa, 270°C, U_0 = 0.6 m/s).

creasing bed porosity increases both conversion and reactor productivity (Figure 2). The operating pressure affects only slightly the conversion.

Hydrogen is responsible for the termination of hydrocarbon chains into paraffins. Increasing the H_2:CO feed ratio increases the partial pressure of H_2 in the reaction media, thus, increasing the termination rate into paraffins. Low H_2:CO ratios maximizes olefin production because the hydrogen concentration is low enough not to terminate all hydrocarbons chains into paraffins. As the H_2:CO ratio increases the termination into paraffin increases, and the ratio of olefin to paraffin tends to zero. Low H_2:CO ratios also favor hydrocarbon chain growth because of the lower termination probability, leading to the production of longer hydrocarbons chains, such as diesel and waxes chains. Higher production of diesel is approximately at a H_2:CO ratio = 0.5, while for gasoline higher production are found at a H_2:CO ratio = 1.0 (Figure 3). Above H_2:CO ratio = 1.0 the production of light gases are favored since an excess of H_2 will terminate the growing chains, leading to the formation of hydrocarbons with low carbon number and low weight. Increasing superficial gas velocity enhances the production of gasoline and diminishes the production of diesel because higher superficial gas velocity adds more syngas into the reactor increasing the partial pressure of the reagents, especially hydrogen that increase chain termination.

The operating pressure changes only slightly the conversion and reactor productivity, but has great effect on chain length. For low-superficial gas velocities, increasing pressure causes an increase in diesel and wax production up to 2.0 MPa, when after that a pressure increase causes a decrease in production

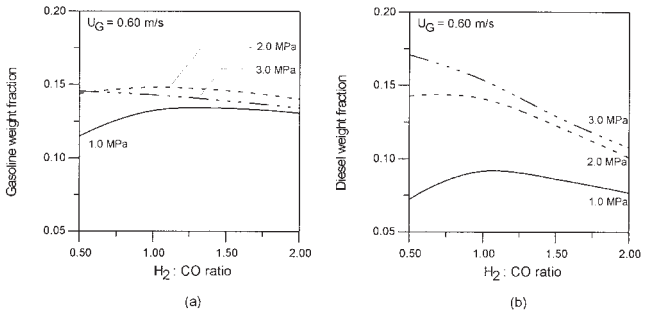

Figure 5. Weight fraction of (a) gasoline; and (b) diesel for three operating pressures (conditions: 270°C, U_0 = 0.6 m/s, ε = 0.85).

(Figures 4 and 5). For gasoline, increasing pressure causes a decrease in production at low-superficial gas velocity, while for high-superficial gas velocity the decrease in production occurs only after 2.0 MPa (Figure 5). Higher pressures favor diesel production, increasing considerably the concentration of CO at the catalyst active site. At low-bed porosity (ε = 0.85) and low-superficial gas velocity (U_0 = 0.4 m/s) diesel production is maximal at 2.0 MPa, but with increasing superficial gas velocities the best operating pressure rises, as does the diesel weight fraction produced. At high-bed porosity (ε = 0.95) high-operating pressures favor diesel production. These results show that the total pressure of the system is a major factor for the operating condition of the reactor.

Increasing catalyst load causes an increase in the overall conversion of syngas, but decreases the conversion of syngas into hydrocarbons by the FT reaction (Figure 2). However, the conversion of carbon monoxide into carbon dioxide and water by the WGS reaction increases steeply. High-catalyst loads, and, therefore, low-bed porosities, diminish the average hydrocarbon chain length due to competitive chain propagation. Increasing catalyst load increases both the amount of active sites available for chain propagation and the competition for the available carbon monoxide and hydrogen in the reaction media, which leads to shorter hydrocarbon chains. As a result, decreasing bed porosity causes a steep decrease in the weight fraction of diesel, especially for bed porosities lower than 0.90 (Figure 6). For gasoline, increasing catalyst load increase the production of gasoline because it favors the reduction in the average hydrocarbon chain length being produced.

The minimum bed porosity where the reactor maintained the isothermal conditions was ε = 0.85. Below this level of bed porosity the reactor temperature increases continuously, and it is not possible to control the temperature of the reactor. This minimum bed porosity is the major disadvantage of the fluidized-bed reactor, since it leads to the need of a large vessel and high-total reactor volume when compared to the slurry-bed reactor,[22] which needs less total vessel volume to achieve the same production. To produce 1 ton/h of gasoline, the fluidized-bed reactor needs to have 202.6 m^3, and a slurry reactor needs to have only 687.7 m^3, for the same amount of catalyst.

Optimization of the FTS was conducted searching for the operating condition that results in the highest production of gasoline and diesel. A program in Fortran was developed in order to maximize the production of these two products using the method of quasi-Newton and a finite-difference gradient.

Table 6. Optimal Operating Conditions for Maximum Yields of Gasoline and Diesel

Optimal Yield of	H_2:CO Ratio	Pressure [MPa]	Bed Porosity	Superficial Gas Velocity [m/s]
Gasoline	1.60	1.0	0.85	0.46
Diesel	0.50	1.7	0.95	0.40

The search for the optimum operating conditions is time-consuming, and the system presents some local maxima that need to be avoided, so several initial estimates for the maximization where used and the best conditions are shown on Tables 6 and 7.

The focus presented herein, is on the maximum yield (maximum mass fraction) of gasoline and diesel, which are the main target products in offshore platforms. Table 6 presents a summary of the optimal operating conditions for maximum yield of gasoline and diesel; and Table 7 presents the production distribution for the optimum conditions for the following optimization problem

Find: P_T, H_2:CO ratio, U_0 and ε_P

Maximize: Product yield (g product/g total hydrocarbon)

$$\max\left\{\Phi = \sum w_i\right\}$$

within ranges of operating conditions (constraints)

$$1.0 \leq P_T \leq 3.0 \text{ MPa}$$

$$0.4 \leq H_2\text{:CO} \leq 3.0$$

$$0.40 \leq U_G \leq 0.60$$

$$0.85 \leq \varepsilon_P \leq 0.95$$

where product is diesel or gasoline.

As shown in Tables 6 and 7, high-concentration of syngas in the reaction media (high-pressure and superficial gas velocity) associated to high-bed porosity and low H_2:CO ratio are the best operating conditions to maximize the yield of diesel in the FTS reaction. Conversion of syngas into diesel can be as high as 21.3% per pass in the reactor, and after recycling of the light gases back to the syngas reformer, the conversion of syngas into diesel is as high as 54.3%. Gasoline production is favored by low-pressure associated to low-bed porosity and high H_2:CO ratio. Conversion of syngas into gasoline can be as high as 14.8% per pass in the reactor, and after recycling of the light gases back to the reformer, the conversion of syngas into gasoline is as high as 46.8%.

Comparing the performance of a slurry reactor using the same kind of catalyst,[22] the yield (mass fraction) of gasoline in the fluidized bed is 13.8% higher than in the slurry reactor at the optimum conditions, making the fluidized-bed reactor a good choice for gasoline production. The total production per m^3 of reactor however is lower. For diesel production the slurry reactor is the best option.

Conclusions

Fischer-Tropsch synthesis can be used to produce transportation fuels from natural gas and the polymerization conditions can be set to maximize the production of a certain product generated by the FTS reaction, such as gasoline and diesel.

From the simulation studies of a fluidized-bed reactor, the optimum operating condition to maximize diesel yield must be under low catalyst load, high-pressure and low-superficial gas velocity, while gasoline is favored by high-catalyst load and low-pressure. High H_2:CO ratios favor production of low-molecular-weight products as gasoline, while low H_2:CO ratios deviate production toward heavy hydrocarbons, such as diesel.

Acknowledgment

The authors gratefully acknowledge the financial support of the Brazilian research funding institution CNPq-CTPetro - Conselho Nacional de Desenvolvimento Científico.

Notation

A = area, m^2
a = equilibrium parameter of the FT reaction rate
$C_{i,j}$ = concentration of component j in phase I, $mol.m^{-3}$
$C_{O,j}$ = initial concentration of component j, $mol.m^{-3}$
Cp_i = heat capacity of component I, $J.mol^{-1}.K^{-1}$
D = diffusivity, $m^2.s^{-1}$
d_b = bubble diameter, m
d_p = catalyst diameter, m
g = gravity, $m.s^{-2}$
H = reactor height, m
Hm_i = heat-transfer coefficient of component I, h^{-1}
k_{et} = ethane formation rate constant, $MPa^{-1}.h^{-1}$
k_{FTS} = overall Fischer-Tropsch rate constant, $mol.kg_{cat}^{-1}.h^{-1}.MPa^{-1}$
k_i = initiation rate constant for the alkyl mechanism, MPa^{-1}
k_{i2} = = initiation rate constant for the alkenyl mechanism, mol^{-1}
k_{met} = methane formation rate constant, $MPa^{-1}.h^{-1}$
k_{O2} = ethylene formation rate constant, $h.mol^{-1}$
k_{olef} = termination by b-elimination rate constant for the alkyl mechanism, h^{-1}
k_{olef2} = termination rate constant for the alkenyl mechanism, h^{-1}
k_p = propagation rate constant for the alkyl mechanism, mol^{-1}
k_{p2} = propagation rate constant for the alkenyl mechanism, mol^{-1}
k_{par} = termination rate constant for the alkyl mechanism yielding paraffin, $MPa^{-1}.h^{-1}$
k_{WGS} = water gas shift reaction rate constant, $mol.kg_{cat}^{-1}.h^{-1}.MPa^{-1}$
K_i = equilibrium constant of reaction i or adsorption coefficient of component i
Km_i = mass-transfer coefficient of component I, h^{-1}
P_i = partial pressure of component I, MPa

Table 7. Product Distribution (Weight Fraction) at the Optimum Conditions for Maximum Yields of Gasoline and Diesel

	Total Paraffin	Olefin	Paraffin Light Gases	LPG	Gasoline	Diesel	Waxes	Diesel HC	Olefin Ethene	Propene	O4+	O15+
Maximum gasoline yield	0.685	0.315	0.294	0.099	**0.148**	0.102	0.041	0.143	0.017	0.068	0.206	0.025
Maximum diesel yield	0.553	0.447	0.147	0.068	0.126	**0.123**	0.090	0.213	0.017	0.072	0.305	0.053

*HC—after hydrocraking of wax fraction.

P_T = total pressure in the reaction zone, MPa
$P(n)$ = paraffin containing n carbons, mol
$P = (n)$ = olefin containing n carbons, mol
R_i = rate of reaction I, $\text{mol.h}^{-1}.\text{kg}_{\text{cat}}^{-1}$
$R(n)$ = alkyl propagating species containing n carbons, mol
$R"n)$ = alkenyl propagating species containing n carbons, mol
R_{FTS} = overall Fischer-Tropsch reaction rate, mol.h^{-1}
R_{WGS} = water gas shift reaction rate, mol.h^{-1}
Re = number of Reynolds
T_j = temperature of phase j, K
U_b = bubbles velocity, m.s^{-1}
U_e = emulsion velocity, m.s^{-1}
V_j = volume of phase j, m^3
V_R = reactor volume, m^3
z = axial position, m
δ = voidage
ϕ = catalyst sphericity
Δ = H heat of reaction, J.mol^{-1}
ε = bed porosity
ν = stoichiometric coefficient
ρ_g = gas density, kg.m^{-3}
ρ_P = catalyst density, kg.m^{-3}
μ_g = gas viscosity

Subscripts

e = emulsion phase
b = bubble phase
mf = minimum fluidizing condition
p = catalyst

Literature Cited

1. Raje AP, Davis BH. Fischer-Tropsch synthesis over iron-based catalysts in a slurry reactor. reaction rates, selectivities and implications for improving hydrocarbon productivity. *Catalysis Today*. 1997;36:335-345.
2. van Steen E, Schulz H. Polymerization kinetics of the Fischer-Tropsch CO hydrogenation using iron and cobalt based catalysts. *Appl Catalysis A*. 1999;186:309-320.
3. Maretto C, Krishna R. Modelling of a bubble column slurry reactor for fischer-tropsch synthesis. *Catalysis Today*. 1999;52:279-289.
4. Krishna R, Sie ST. Design and scale up of the fischer-tropsch bubble column slurry reactor. *Fuel Processing Technol*. 2000;64:73-105.
5. Krishna R, van Baten JM, Urseanu MI, Ellenberger J. Design and scale up of a bubble column slurry reactor for fischer-tropsch synthesis. *Chem Eng Sci*. 2001;56:537-545.
6. Wang YN, Xu YY, Li YW, Zhao YL, Zhang BJ. Heterogeneous modeling for fixed bed fischer-tropsch synthesis: reactor model and its applications. *Chem Eng Sci*. 2003;58:867-875.
7. Knottenbelt C. Mossgas "gas-to-liquid" diesel fuels - an environmentally friendly option. *Catalysis Today*. 2002;71:437-445.
8. Wilhelm DJ, Simbeck DR, Karp AD, Dickenson RL. Syngas production for gas-to-liquids applications: technologies, issues and outlook. *Fuel Process Technol*. 2001;71:139-148.
9. Huff GA, Satterfield CN. Evidence for two chain growth probabilities on iron catalysts in the Fischer-Tropsch synthesis. *J of Catal*. 1984; 85:370-379.
10. Iglesia E, Reyes SC, Madon RJ. Transport-enhanced α-olefin readsorption pathways in Ru-catalyzed hydrocarbon synthesis. *J of Catal*. 1991;129:238-256.
11. Madon RJ, Taylor WF. Fischer-Tropsch synthesis on a precipitated iron catalyst. *J of Catal*. 1981 69:32-43.
12. Patzlaff J, Liu Y, Graffmann C, Gaube J. Studies on product distributions of iron and cobalt catalyzed Fischer-Tropsch synthesis. *Appl Catal A*. 1999;186:109-117.
13. Patzlaff J, Liu Y, Graffmann C, Gaube J. Interpretation and kinetic modeling of product distributions of cobalt catalyzed fischer-tropsch synthesis. *Catalysis Today*. 2002;71:381-394.
14. Lucas A, Arnaldos J, Casal J, Puigjaner L. Improved equation for the calculation of minimum fluidization velocity. *Ind and Eng Cheml Proc Design and Development*. 1986;25:426-429
15. Bukul DB, Nasif N, Daly JG. On the use of effective bubble diameters in the countercurrent backmixing model for fluid bed reactors. Chem Eng Sci. 1974;42:1510-1513.
16. Davidson JF, Harrison D. *Fluidized Particles.* New York: Cambridge University Press; 1963.
17. Kunii D, Levenspiel O. *Fluidization Engineering*. New York: Wiley Press; 1969.
18. Broadhurst TE, Becker HA. Onset of fluidization and slugging in beds of uniform particles. *AIChE J*. 1975;21:238-247.
19. Mori S, Wen CY. Estimation of bubble diameter in gaseous fluidized beds. *AIChE J*. 1975;21:109-115.
20. Fernandes FAN. Polymerization kinetics of Fischer-Tropsch reaction on iron based catalysts and product grade optimization. *Chem Eng & Technol*. 2005;28:930-938.
21. Donnelly TJ, Satterfield CN. Product distributions of the Fischer-Tropsch synthesis on precipitated iron catalysts. *Appl Catal*. 1989; 52:93.
22. Fernandes, FAN. Modeling and product grade optimization of Fischer-Tropsch synthesis in a slurry reactor. *Ind and Eng Chem Res*. 2006; 45:1047.

Manuscript received Aug. 19, 2005, and revision received Mar. 29, 2006.